Bol. Soc. Paran. Mat.
©SPM – E-ISSN-2175-1188
SPM: www.spm.uem.br/bspm

(3s.) **v. 2025 (43)** : 1–15.
ISSN-0037-8712
doi:10.5269/bspm.76751

Dynamic Interactions Between HIV-1 and Cancer: Hopf Bifurcation and Stability in a Dual Time-Delay Mathematical Model

Rukiye Kara

ABSTRACT: The objective of this paper is to extend an existing mathematical model of HIV-associated cancer by incorporating two critical time delays: one between viral entry into a cell and the onset of latency and the other between cell infection and the start of viral production. By performing a Hopf bifurcation analysis, we examined four different scenarios to gain insight into how these delays contribute to oscillatory behaviors and periodic solutions in cell populations. The results of numerical simulations demonstrate the impact of these delays on the stability of healthy and infected cells and highlight the importance of infected T cells in the progression of AIDS-related complications.

Key Words: Mathematical model, stability analysis, Hopf bifurcation, numerical simulation.

Contents

1. Introduction

According to a recent study, HIV infections negatively impact the immune system. The kidneys, brain, and heart are just a few critical organs that could sustain serious harm from this. For those who are HIV positive, the increased risk of cancer is a major concern. Kaposi's sarcoma is the most common tumor seen in AIDS patients (KS). This group is often affected by AIDS-KS, a syndrome that frequently presents itself. Tumors on the skin or mucosa, with a preference for the oral mucosa, are the hallmark of the malignant Kaposi's sarcoma (KS). It originates from cells lining the blood or lymphatic vessels. However, these tumors can also arise in other regions of the body, such as the lymph nodes, lungs, and digestive tract [1]. In addition, another important condition, intermediate and high-grade non-Hodgkin lymphomas (NHLs), is recognized as a disease that characterizes AIDS. Human immunodeficiency virus (HIV) positive individuals often exhibit unusual manifestations of both Hodgkin's disease and non-Hodgkin lymphoma (NHL) [8].

Significant progress has been made in using mathematical models to improve our comprehension of the dynamics of viral infections, such as HIV-1. Investigating the dynamics of biological systems and infectious diseases requires the use of such models, as they are highly beneficial in clarifying the intricacies of biological processes and providing in-depth insights into the mechanisms underlying these systems [3,4,6,5]. For instance, the stability of within-host viral dynamics models that account for infection process delays has been investigated [11]. A mathematical analysis is employed to determine the conditions under which the infection either remains stable or becomes unstable. A mathematical model that accounts for treatment efficacy differences and delays in the infection process was used in [10] to study the global dynamics of HIV infection. To determine the prerequisites for stability and global dynamics, the study conducts a thorough investigation. [7] investigated the chaotic dynamics of an HIV-1-related cancer model. A mathematical analysis of within-host virus models, including cell-to-cell viral transmission, is described in [12]. The goal of the research is to gain insight into the global dynamics of these models, with an emphasis on determining the conditions under which the virus either persists or

Submitted May 12, 2025. Published August 24, 2025
2020 *Mathematics Subject Classification:* 34A34, 37N25, 37N30.

is eradicated. In [13], a mathematical model was constructed to describe the dynamics of HIV infection within CD4+ T cells. This model captures the interaction between the virus and the immune system, particularly focusing on how the virus infects and depletes CD4+ T cells. In [14], a delay-differential equation model is introduced to describe the dynamics of HIV infection in CD4+ T cells. This model incorporates delays to account for the time lag in the viral replication cycle and the immune response.

One of the in vivo transmission routes of HIV-1 is the transfer of HIV-infected T cells to healthy T cells. Numerous studies have investigated the mechanisms of HIV transmission and regulation, emphasizing the critical roles of cell-to-cell transmission, immune cell interactions, and factors affecting viral production and steady-state viral loads [15,16,17,18]. In their studies, Lou et al. examine the intricate interactions between HIV-1 and cancer within infected individuals. They present a mathematical model incorporating time delays to study the dynamics of AIDS-related cancer [7,8]. [9] present a mathematical model using delay-differential equations to describe the interactions between HIV, cancer, and the immune system. Duarte et al. investigate the potential of optimal homotopy analysis methods for analyzing a chaotic mathematical model of HIV-1 dynamics, which incorporates interactions with AIDS-related cancer cells [19].

This study aims to investigate how HIV-1 spreads from cell to cell in tissues containing cancer cells. We employ a two-time-delay mathematical model, building upon the framework established by [19]. Our model incorporates the crucial 'incubation' period of HIV, recognizing that the time between viral infection and new virus production varies. While actively infected CD4+ T cells typically release new virus within 24 hours, quiescent lymphocytes can retain the virus for up to 60 days [20]. This research underscores the significance of the incubation phase in both HIV infection and cancer progression, emphasizing the diverse incubation periods of different target cells.

Additionally, we explore the potential for complex behavior in our HIV-cancer model by investigating Hopf bifurcations. We analyze how time delays can lead to oscillations in the model's variables. To do this, we examine the stability of the equilibrium point and determine the conditions under which it loses stability, giving rise to periodic solutions. Our findings are supported by computer simulations.

2. HIV-1 Related Cancer Model with Two Delays

To better understand the complex dynamics between HIV-1 and cancer, we've expanded the HIV-cancer model introduced by [7] to include two time delays. These delays account for the crucial incubation period between initial viral exposure and the ability to transmit the virus. In the case of HIV, this involves the time it takes for a healthy cell to become infected and then infectious.

The immune system is adept at distinguishing between healthy and cancerous cells, targeting the latter for destruction. CD4+ T lymphocytes are key players in this defense, representing the immune system's frontline in our model. These cells not only kill cancer cells upon contact but can also interfere with the spread of cancer by interacting with other cancer cells.

Our study focuses on understanding how HIV infection impacts cancer development. To model this, we track the populations of cancer cells ($x(t)$), healthy cells ($y(t)$), and HIV-infected cells ($z(t)$) over time.

$$\begin{aligned}
\frac{dx(t)}{dt} &= x(t)\Big[a_1\Big(1-\frac{x(t)+y(t)+z(t)}{m}\Big)-b_1y(t)\Big]\\
\frac{dy(t)}{dt} &= y(t)\Big[a_2\Big(1-\frac{x(t)+y(t)+z(t)}{m}\Big)-pb_1x(t)-b_2z(t)\Big]\\
\frac{dz(t)}{dt} &= b_2y(t-\tau_1)z(t-\tau_2)-dz(t)
\end{aligned} \tag{2.1}$$

with the initial condition

$$x(0)=x_0,\quad y(0)=y_0,\quad z(0)=z_0. \tag{2.2}$$

We assume that cancer originates from a single cell due to gene mutation and use the parameter a_1 to represent the uncontrolled proliferation rate of cancer cells. b_1 is the immune system's killing rate of cancer cells, m is the effective carrying capacity of the system, a_2 is the intrinsic growth rate of healthy

cells, and p represents the rate of loss due to immune cells killing cancer cells. b_2 is the HIV-1 infection rate coefficient, representing the rate at which healthy cells convert to infected cells, while d is the immune system's killing rate of infected cells. τ_1 is the delay in the impact of infected cells on healthy cells, and τ_2 is the delay in the interaction of healthy cells with infected cells. The infection process of infected and healthy cells is described by the term $b_2y(t)z(t)$.

The growth of the populations for the cancer and the immune system cells is limited by a logistic-like function, given by $1-\frac{x+y+z}{m}$. This function introduces competition between the cancer cells and both the healthy and infected T-cells.

In this study, we deal with only the cancer-HIV-healthy steady state. The equilibrium points of the system satisfy $x(t)=x^*$, $y(t)=y(t-\tau_1)=y^*$, and $z(t)=z(t-\tau_2)=z^*$. These points are determined by the following set of equations

$$0 = x(t)\Big[a_1\Big(1-\frac{x(t)+y(t)+z(t)}{m}\Big)-b_1y(t)\Big] \tag{2.3}$$

$$0 = y(t)\Big[a_2\Big(1-\frac{x(t)+y(t)+z(t)}{m}\Big)-pb_1x(t)-b_2z(t)\Big] \tag{2.4}$$

$$0 = b_2y(t-\tau_1)z(t-\tau_2)-dz(t). \tag{2.5}$$

By solving the above system, one of the equilibrium points, the cancer-HIV-healthy steady state, is represented by $E^*(x^*,y^*,z^*)$, which is computed as follows

$$x^* = \frac{a_2b_1d+mb_1b_2d+a_1b_2d-ma_1b_2^2}{a_1b_2(pb_1-b_2)} \tag{2.6}$$

$$y^* = \frac{d}{b_2} \tag{2.7}$$

$$z^* = \frac{ma_1b_1b_2p-da_1b_1p-mb_1^2dp-a_2b_1d}{a_1b_2(pb_1-b_2)}. \tag{2.8}$$

To guarantee the existence of a biologically meaningful equilibrium point where all cell populations remain positive, the following conditions must be fulfilled,

- $\frac{a_1p(mb_2-1)}{d(a_2+pmb_1)}<1$,
- $\frac{a_1b_2(mb_2-d)}{b_1d(a_2+mb_2)}>1$.

Additionally, we assume $pb_1\neq b_2$ to avoid division by zero in the expressions for the equilibrium points x^* and y^*, given in equations (2.6) and (2.8). This assumption is necessary to ensure that these expressions are well-defined and that the equilibrium is valid.

To explore the system's qualitative behavior without explicitly solving the equations, we derive the characteristic equation. This equation provides insights into the system's dynamics around its equilibrium points. We start by calculating the Jacobian matrices of the system evaluated at the equilibrium point E^*,

$$J=\begin{bmatrix} a_1\Big(1-\frac{2x^*+y^*+z^*}{m}\Big)-b_1y^* & -x^*\Big(\frac{a_1}{m}+b_1\Big) & -\frac{a_1}{m}x \\ -y^*\Big(\frac{a_2}{m}+pb_1\Big) & a_2\Big(1-\frac{x^*+2y^*+z^*}{m}\Big)-pb_1x^*-b_2z^* & -y^*\Big(\frac{a_2}{m}+b_2\Big) \\ 0 & 0 & -d \end{bmatrix},$$

$$J_{\tau_1}=\begin{bmatrix}0&0&0\\0&0&0\\0&b_2z^*&0\end{bmatrix},\quad J_{\tau_2}=\begin{bmatrix}0&0&0\\0&0&0\\0&0&b_2y^*\end{bmatrix}.$$

The corresponding characteristic equation of the system is

$$\det(J + e^{-\lambda\tau_1}J_{\tau_1} + e^{-\lambda\tau_2}J_{\tau_2} - \lambda I) = \lambda^3 + A_2\lambda^2 + A_1\lambda + A_0 + (B_1\lambda + B_0)e^{-\lambda\tau_1} + (C_2\lambda^2 + C_1\lambda + C_0)e^{-\lambda\tau_2} = 0 \tag{2.9}$$

where

$$\begin{aligned}
A_2 &= d + \frac{a_2y^*}{m} + \frac{a_1x^*}{m},\\
A_1 &= d\Big(\frac{a_2y^*}{m} + \frac{a_1x^*}{m}\Big) - \Big(\frac{a_2}{m} + \frac{a_1p}{m} + pb_1\Big)b_1x^*y^*,\\
A_0 &= -\Big(\frac{a_2}{m} + \frac{a_1p}{m} + pb_1\Big)b_1dx^*y^*,\\
B_1 &= b_2\Big(\frac{a_2}{m} + b_2\Big)y^*z^*,\\
B_0 &= \frac{a_1b_2}{m}(b_2 - pb_1)x^*y^*z^*,\\
C_2 &= -b_2y^*,\\
C_1 &= -b_2y^*\Big(\frac{a_2y^*}{m} + \frac{a_1x^*}{m}\Big),\\
C_0 &= \Big(\frac{a_2}{m} + \frac{a_1p}{m} + pb_1\Big)b_1b_2x^*y^{*2}.
\end{aligned}$$

We will consider four cases: ***i)*** $\tau_1 = \tau_2 = 0$, ***ii)*** $\tau_1 > 0$, $\tau_2 = 0$, ***iii)*** $\tau_1 = 0$, $\tau_2 > 0$, ***iv)*** $\tau_1 \neq \tau_2 \neq 0$.

Case I: $\tau_1 = \tau_2 = 0$ In this case, the characteristic equation becomes:

$$P(\lambda) = \lambda^3 + D_2\lambda^2 + D_1\lambda + D_0,$$

where

$$D_2 = A_2 + C_2, \quad D_1 = A_1 + B_1 + C_1, \quad \text{and} \quad D_0 = A_0 + B_0 + C_0.$$

Using the Routh-Hurwitz criterion, we determine that the system is locally asymptotically stable at the equilibrium point E^* when the conditions $D_2 > 0$, $D_0 > 0$, and $D_1D_2 - D_0 > 0$ are satisfied. Clearly, $D_2 > 0$, and $D_0 > 0$ holds if $b_2 > pb_1$. To ensure that $D_1D_2 - D_0$ remains positive, the following inequality must hold,

$$d\Big(\frac{a_2y^*}{m} + \frac{a_1x^*}{m}\Big)z^* > \Big(\frac{a_2}{m} + \frac{a_1p}{m} + pb_1\Big)\Big(\frac{a_2y^*}{m} + \frac{a_1x^*}{m}\Big)b_1x^*y^* + \frac{a_2d}{m}(b_2 - pb_1)x^*z^*.$$

Consequently, when $\tau_1 = \tau_2 = 0$, the system is locally asymptotically stable around the equilibrium point E^*.

Case II: $\tau_1 > 0$, $\tau_2 = 0$ In this case, we consider a scenario where $\tau_1 > 0$ and $\tau_2 = 0$, analyzing the impact of a single time delay (τ_1) on the system dynamics. The characteristic equation then takes the form,

$$P(\lambda, \tau_1) = \lambda^3 + E_2\lambda^2 + E_1\lambda + E_0 + (B_1\lambda + B_0)e^{-\lambda\tau_1}, \tag{2.10}$$

where

$$E_2 = A_2 + C_2, \quad E_1 = A_1 + C_1, \quad \text{and} \quad E_0 = A_0 + C_0 = 0.$$

Theorem 2.1 *The system is locally asymptotically stable at equilibrium point E^* for delay value τ_1 in the interval $[0, \tau_1^*)$, while $\tau_2 = 0$. However, the system becomes unstable when the delay τ_1 exceeds the critical value τ_1^*.*

Proof: If $\lambda = i\omega$ is one of the roots of $P(\lambda, \tau_1)$, by substituting $\lambda = i\omega$ into the characteristic equation (2.10) and separating the real and imaginary parts, we obtain the following system of equations,

$$B_0 \cos(\omega\tau_1) + B_1\omega \sin(\omega\tau_1) = E_2\omega^2, \tag{2.11}$$

$$-B_0 \sin(\omega\tau_1) + B_1\omega \cos(\omega\tau_1) = \omega^3 - E_1\omega. \tag{2.12}$$

Squaring both equations and summing them yields,

$$\omega^6 + \omega^4(E_2^2 - 2E_1) + \omega^2(E_1^2 - B_1^2) - B_0^2 = 0. \tag{2.13}$$

For the positive root, let introduce new variable $z = \omega^2$, then we have,

$$h_1(z) = z^3 + z^2(E_2^2 - 2E_1) + z(E_1^2 - B_1^2) - B_0^2 = 0. \tag{2.14}$$

We seek a positive real root for the equation in z. Clearly, B_0^2 is positive and represents the product of the equation's roots. Furthermore,

$$E_2^2 - 2E_1 = \Big(\frac{a_2 y^*}{m} + \frac{a_1 x^*}{m}\Big)^2 + 2\Big(\frac{a_2}{m} + \frac{a_1 p}{m} + p b_1\Big) b_1 x^* y^* > 0,$$

which is equal to the sum of roots of $h_1(z)$. So, $h_1(0) < 0$ and $\lim_{z\to\infty} h_1(z) = \infty$. Notice that

$$h_1'(z) = 3z^2 + 2(E_2^2 - 2E_1)z + E_1^2 - B_1^2. \tag{2.15}$$

Since $E_2^2 - 2E_1 > 0$, $h_1'(z)$ has at most only one positive root, regardless of whether $E_1^2 - B_1^2 > 0$ or $E_1^2 - B_1^2 < 0$. Consequently, Eq. (2.13) has at most one positive root, denoted by ω_0, which corresponds to a pair of purely imaginary roots, $\pm i\omega_0$, for the characteristic equation (2.10).

From Equations (2.11), we get

$$\cos(\omega\tau_1) = \frac{B_1\omega^4 + (B_0E_2 - B_1E_1)\omega^2}{B_0^2 + B_1^2\omega^2}, \tag{2.16}$$

and

$$\sin(\omega\tau_1) = \frac{(B_1E_2 - B_0)\omega^3 + B_0E_1\omega}{B_0^2 + B_1^2\omega^2}. \tag{2.17}$$

Equation (2.16) yields,

$$\tau_{1,j} = \frac{1}{\omega_0}\arccos\Big(\frac{B_1\omega_0^4 + (B_0E_2 - B_1E_1)\omega_0^2}{B_0^2 + B_1^2\omega_0^2}\Big) + \frac{2\pi j}{\omega_0}, \quad j = 0, 1, 2, \ldots \tag{2.18}$$

For $j = 0$, it can be taken as $\tau_1^* = \tau_{1,0}$.

Additionally, we verify the transversality condition:

$$\frac{d}{d\tau_1}\Re e\Big[\lambda(\tau_1)\Big]\Big|_{\tau_{1,0}} \neq 0. \tag{2.19}$$

Assuming $\lambda(\tau_1) = v(\tau_1) + i\omega(\tau_1)$ is a solution of (2.10), we find that $v(\tau_{1,0}) = 0$ and $\omega(\tau_{1,0}) = \omega_0$. Differentiating Equation (2.10) with respect to τ_1 yields,

$$\Big(\frac{d\lambda}{d\tau_1}\Big)^{-1} = \frac{(3\lambda^2 + 2E_2\lambda + E_1)e^{\lambda\tau_1}}{B_0\lambda + \lambda^2 B_1} + \frac{B_1}{B_0\lambda + B_1\lambda^2} - \frac{\tau_1}{\lambda}. \tag{2.20}$$

We know that when $\tau_1 = \tau_{1,0}$, $\lambda = i\omega_0$. Therefore, we have,

$$\Re e\left\{\Big(\frac{d\lambda}{d\tau_1}\Big)^{-1}\right\} = \frac{\beta_1\cos(\omega_0\tau_1) + \beta_2\sin(\omega_0\tau_1) - B_1^2\omega_0^2}{B_1^2\omega_0^4 + B_0^2\omega_0^2}, \tag{2.21}$$

where

$$\beta_1 = 3B_1\omega_0^4 + (-B_1E_1 + 2E_2B_0)\omega_0^2,$$
$$\beta_2 = (2E_2B_1 - 3B_0)\omega_0^3 + E_1B_0\omega_0.$$

$$\Re e\left\{\left(\frac{d\lambda}{d\tau_1}\right)^{-1}\right\} = \frac{1}{(B_1^2\omega_0^2 + B_0^2)^2}\Big(3B_1^2\omega_0^6 + (2B_1^2E_2^2 + 3B_0^2 - 4B_1^2E_1)\omega_0^4 + (2B_0^2E_2^2 + B_1^2E_1^2 - 4B_0^2E_1)\omega_0^2 + B_0^2E_1^2\Big). \tag{2.22}$$

Since $E_1 < 0$, it follows that the sign of $\Re e\left\{\left(\frac{d\lambda}{d\tau_1}\right)^{-1}\right\}$ is positive. Consequently, the transversality condition is satisfied. A Hopf bifurcation occurs as τ_1 surpasses the critical value $\tau_{1,0}$. □

Case III: $\tau_1 = 0$, $\tau_2 > 0$ In this case, we focus on the scenario where $\tau_1 = 0$ and $\tau_2 > 0$, examining the effect of the second time delay (τ_2) on the system's behavior. The characteristic equation is then expressed as,

$$P(\lambda, \tau_2) = \lambda^3 + F_2\lambda^2 + F_1\lambda + F_0 + (C_2\lambda^2 + C_1\lambda + C_0)e^{-\lambda\tau_2} = 0, \tag{2.23}$$

where

$$F_2 = A_2,$$
$$F_1 = A_1 + B_1,$$
$$F_0 = A_0 + B_0.$$

Theorem 2.2 *The system is locally asymptotically stable at equilibrium point E^* for delay values τ_2 in the interval $[0, \tau_2^*)$ when $\tau_1 = 0$. However, the system becomes unstable when the delay τ_2 exceeds the critical value τ_2^*.*

Proof: Let $\lambda = i\omega$ be a root of Eq. (2.23), then we have the following pair of equations:

$$(C_0 - C_2\omega^2)\cos(\omega\tau_2) + C_1\omega\sin(\omega\tau_2) = F_2\omega^2 - F_0, \tag{2.24}$$
$$(-C_0 + C_2\omega^2)\sin(\omega\tau_2) + C_1\omega\cos(\omega\tau_2) = \omega^3 - F_1\omega. \tag{2.25}$$

Taking the square and summation, we obtain:

$$\omega^6 + (F_2^2 - 2F_1 - C_2^2)\omega^4 + (F_1^2 - 2F_0F_2 + 2C_0C_2 - C_1^2)\omega^2 + F_0^2 - C_0^2 = 0. \tag{2.26}$$

We are looking for positive ω, so suppose $z = \omega^2$,

$$h_2(z) = z^3 + (F_2^2 - 2F_1 - C_2^2)z^2 + (F_1^2 - 2F_0F_2 + 2C_0C_2 - C_1^2)z + F_0^2 - C_0^2 = 0. \tag{2.27}$$

To find positive roots of the equation, we observe that the product of the roots is positive when $F_0^2 - C_0^2 = B_0(B_0 + 2A_0) < 0$. Consequently, $h_2(0) < 0$ and $\lim_{z\to\infty} h_2(z) = \infty$. Therefore, Equation (2.27) has at least one positive root and Eq. (2.26) has at least one positive root, denoted ω_0.

From Equations (2.24), we get:

$$\cos(\omega\tau_2) = \frac{(C_1 - F_2C_2)\omega^4 + (F_2C_0 + F_0C_2 - F_1C_1)\omega^2 - F_0C_0}{(C_0 - C_2\omega^2)^2 + C_1^2\omega^2}, \tag{2.28}$$

$$\sin(\omega\tau_2) = \frac{C_2\omega^5 + (F_2C_1 - C_0 - F_1C_2)\omega^3 - (F_0C_1 - F_1C_0)\omega}{(C_0 - C_2\omega^2)^2 - C_1^2\omega^2}, \tag{2.29}$$

and

$$\tau_{2,j} = \frac{1}{\omega_0}\arccos\left(\frac{(C_1 - F_2C_2)\omega_0^4 + (F_2C_0 + F_0C_2 - F_1C_1)\omega_0^2 - F_0C_0}{(C_0 - C_2\omega_0^2)^2 + C_1^2\omega_0^2}\right) + \frac{2\pi j}{\omega_0}. \tag{2.30}$$

For $j = 0$, it can be taken as $\tau_2^* = \tau_{2,0}$.
To verify the transversality condition, we calculate:

$$\left(\frac{d\lambda}{d\tau_2}\right)^{-1} = \frac{3\lambda^2 + 2F_2\lambda + F_1}{\lambda(C_2\lambda^2 + C_1\lambda + C_0)}e^{\lambda\tau_2} + \frac{2C_2\lambda + C_1}{\lambda(C_2\lambda^2 + C_1\lambda + C_0)} - \frac{\tau_2}{\lambda}. \tag{2.31}$$

Evaluating this expression at $\tau_2 = \tau_{2,0}$ and $\lambda = i\omega_0$, we obtain:

$$\Re e\left\{\left(\frac{d\lambda}{d\tau_2}\right)^{-1}\right\} = \frac{\beta_3\cos(\omega_0\tau_2) + \beta_4\sin(\omega_0\tau_2) + C_1C_0 + 2C_2\omega_0^2(C_1\omega_0 - C_2\omega_0^3)}{C_0^2 + (C_1\omega_0 - C_2\omega_0^3)^2}, \tag{2.32}$$

where

$$\begin{aligned}\beta_3 &= C_0(F_1 - 3\omega_0^2) + 2F_2\omega_0(-C_2\omega_0^3 + C_1\omega_0),\\ \beta_4 &= (C_1\omega_0 - C_2\omega_0^3)(-3\omega_0^2 + F_1) - 2C_0F_2\omega_0.\end{aligned}$$

The transversality condition holds if

$$\beta_3\cos(\omega_0\tau_2) + \beta_4\sin(\omega_0\tau_2) + C_1(C_0 - C_1\omega_0^2) - 2C_2^2\omega^4 \neq 0.$$

This ensures that $\Re e\left\{\left(\frac{d\lambda}{d\tau_2}\right)^{-1}\right\} \neq 0$. □

Under different delay parameters, Theorems 2.2 and 2.1 investigate the model's local stability. Since a characteristic equation analysis is performed in both theorems, the methods of proof are comparable. Nonetheless, the two theorems describe different dynamics since they concentrate on situations in which the delay parameters vary. The case where $\tau_1 > 0$ and $\tau_2 = 0$ is covered by Theorem 2.1, whereas $\tau_1 = 0$ and $\tau_2 > 0$ are covered by Theorem 2.2. Different stability conditions within the system result from each of these scenarios.

Case IV: $\tau_1 \neq \tau_2 \neq 0$ In this case, we analyze the scenario where both time delays are non-zero, with τ_1 treated as a variable parameter while τ_2 is kept fixed within the interval $(0, \tau_2^*)$, where τ_2^* is any real number.

Theorem 2.3 *For a fixed τ_2 within the interval $(0, \tau_2^*)$ where τ_2^* is any real number, the equilibrium point E^* of the system is locally asymptotically stable when τ_1 lies within the interval $(0, \tau_{1,0}^*)$. A Hopf bifurcation occurs at the system when τ_1 exceeds the critical value $\tau_{1,0}^*$.*

Proof: By substituting $\lambda = i\omega$ into the characteristic equation (2.10), we obtain,

$$\begin{aligned}P(i\omega, \tau_1, \tau_2) = &-i\omega^3 - A_2\omega^2 + iA_1\omega + A_0 + (iB_1\omega + B_0)e^{-i\omega\tau_1}\\ &+ (-C_2\omega^2 + iC_1\omega + C_0)e^{-i\omega\tau_2}.\end{aligned} \tag{2.33}$$

Separating the real and imaginary parts yields,

$$B_1\omega\cos(\omega\tau_1) - B_0\sin(\omega\tau_1) = \omega^3 - A_1\omega + (C_0 - C_2\omega^2)\sin(\omega\tau_2) - C_1\omega\cos(\omega\tau_2), \tag{2.34}$$

$$B_1\omega\sin(\omega\tau_1) + B_0\cos(\omega\tau_1) = A_2\omega^2 - A_0 - (C_0 - C_2\omega^2)\cos(\omega\tau_2) - C_1\omega\sin(\omega\tau_2). \tag{2.35}$$

Squaring and summing these equations results in

$$G(\omega,\tau_1)=\omega^6+p_5\omega^5+p_4\omega^4+p_3\omega^3+p_2\omega^2+p_1\omega+p_0=0, \tag{2.36}$$

where

$$p_5=-2C_2\sin(\omega\tau_2), \tag{2.37}$$
$$p_4=-2A_1+C_2^2+A_2^2+2(A_2C_2-C_1)\cos(\omega\tau_2), \tag{2.38}$$
$$p_3=2(C_0+A_1C_2-A_2C_1)\sin(\omega\tau_2), \tag{2.39}$$
$$p_2=A_1^2-B_1^2+C_1^2-2A_0A_2-2C_0C_2+2(A_1C_1-A_2C_0-A_0C_2)\cos(\omega\tau_2), \tag{2.40}$$
$$p_1=2(-A_1C_0+A_0C_1)\sin(\omega\tau_2), \tag{2.41}$$
$$p_0=A_0^2-B_0^2+C_0^2+2A_0C_0\cos(\omega\tau_2). \tag{2.42}$$

By applying Descartes' rule of signs, we can determine that Equation (2.36) has at least one positive root ω_0, if the following condition holds,

$$-2A_1+C_2^2+A_2^2+2(A_2C_2-C_1)\cos(\omega\tau_2)<0. \tag{2.43}$$

This condition arises from the fact that $p_5=-2C_2\sin(\omega\tau_2)>0$.

From Equations (2.34), we obtain following expressions.

$$\begin{aligned}\cos(\omega_0\tau_1)=\frac{1}{B_1^2\omega^2+B_0^2}\Big(&B_1\omega_0^4-(A_1B_1-A_2B_0)\omega^2-A_0B_0\\&+(B_1C_0\omega-B_1C_2\omega^3-B_0C_1\omega)\sin(\omega\tau_2)\\&-(B_1C_1\omega^2+B_0C_0-B_0C_2\omega^2)\cos(\omega\tau_2)\Big),\end{aligned} \tag{2.44}$$

$$\begin{aligned}\sin(\omega\tau_1)=\frac{1}{B_1^2\omega^2+B_0^2}\Big(&(A_2B_1-B_0)\omega^3+(A_1B_0-A_0B_1)\omega\\&+(-B_0C_0+B_0C_2\omega^2-B_1C_1\omega^2)\sin(\omega\tau_2)\\&+(B_0C_1\omega-B_1C_0\omega+B_1C_2\omega^3)\cos(\omega\tau_2)\Big).\end{aligned} \tag{2.45}$$

Consequently, using (2.44) we can express $\tau_{1,0}^*$ as:

$$\tau_{1,0}^*=\frac{1}{\omega_0}\arccos\left(\frac{P}{B_1^2\omega^2+B_0^2}\right)+\frac{2\pi j}{\omega_0}, \tag{2.46}$$

where:

$$\begin{aligned}P=&B_1\omega^4-(A_1B_1-A_2B_0)\omega^2-A_0B_0\\&+(B_1C_0\omega-B_1C_2\omega^3-B_0C_1\omega)\sin(\omega\tau_2)\\&-(B_1C_1\omega^2+B_0C_0-B_0C_2\omega^2)\cos(\omega\tau_2).\end{aligned}$$

To verify the transversality condition, we get

$$\Re e\left\{\left(\frac{d\lambda}{d\tau_1}\right)^{-1}\right\}=\frac{Q_1-Q_2}{Q_3}, \tag{2.47}$$

where

$$
\begin{aligned}
Q_1 &= \cos(\omega_0\tau_1)\Big(3B_1\omega_0^4 + 2B_0A_2\omega^2\Big) + \sin(\omega_0\tau_1)\Big(2A_1B_1\omega^3 + A_1B_0\omega_0\Big) \\
&\quad + \cos((\tau_1-\tau_2)\omega_0)\Big(2B_0C_2\omega_0^2 + \tau_2B_1C_0\omega_0^2\Big) \\
&\quad + \sin((\tau_1-\tau_2)\omega_0)\Big(2B_1C_1\omega_0^3 + B_0C_1\omega_0 + \tau_2B_0C_2\omega_0^3\Big), \\
Q_2 &= \cos(\omega_0\tau_1)A_1B_1\omega_0^2 + 3\sin(\omega_0\tau_1)B_0\omega_0^3 \\
&\quad + \cos(\omega_0(\tau_1-\tau_2))\Big(B_1C_1\omega_0^2 + \tau_2(B_1C_2\omega_0^4 + B_0C_1\omega_0^2)\Big) \\
&\quad + \tau_2\sin(\omega_0(\tau_1-\tau_2))\Big(B_1C_1\omega_0^3 + B_0C_0\omega_0\Big) + B_1^2\omega_0^2, \\
Q_3 &= B_1^2\omega_0^4 + B_0^2\omega_0^2.
\end{aligned}
$$

If $Q_1 - Q_2 \neq 0$, then the transversality condition $\Re e\left\{\left(\frac{d\lambda}{d\tau_1}\right)^{-1}\right\} \neq 0$ holds, and a Hopf bifurcation occurs for $\tau_1 = \tau_{1,0}^*$. □

3. Numerical Simulations

This section presents numerical simulations to validate the theoretical Hopf bifurcation analysis of the system defined by equations (2.1). To illustrate the theoretical findings, the dynamics of the system is explored numerically using the parameter values in Table 1. These parameter values were selected based on their use in previous models of similar phenomena or experimental data.

Table 1: Parameter values used in the simulation and corresponding references.

Parameters	Range Values	Unit	References
a_1	$0.05 - 0.5$	day	[21]
a_2	0.03	day	[13]
b_1	$10^{-5} - 10^{-3}$	ml/day	[13]
b_2	$10^{-5} - 5\times10^{-3}$	ml/day	[22]
m	1500	ml	[23]
d	0.3	day	[14]
p	0.1	-	[21]

For the numerical simulation, referring to the parameter values in the Table 1, we use the following values

$$a_1 = 0.12, \quad a_2 = 0.03, \quad b_1 = 0.0001, \quad b_2 = 0.0005, \quad p = 0.1, \quad d = 0.3, \quad m = 1500.$$

. Initial conditions are taken as

$$x_0 = 1, \quad y_0 = 800, \quad z_0 = 10.$$

. The calculated positive equilibrium point is $E^*(122.448979, 600.0, 27.551020)$. Based on the stability criteria for Case I ($D_1 = 0.0040188$, $D_2 = 0.021796$ and $D_1D_2 - D3 = 4.7919\times10^{-05} > 0$), the equilibrium point E^* is asymptotically stable when $\tau_1 = \tau_2 = 0$ as illustrated in Figure 1.

In accordance with Theorem 2.1, the transversality condition for the Hopf bifurcation of the cancer-HIV model is satisfied since $E_1 = -0.000279$. The critical value of τ_1 is calculated as 2.720764, with a corresponding ω_0 value of 0.06205, while τ_2 remains fixed at zero. Furthermore, when the value of τ_1 is less than the critical value $\tau_{1,0}$, which is equal to 2.720764 , the equilibrium point E^* is asymptotically stable. This is demonstrated in Figures 2-3. If the value of τ_1 is equal to $\tau_{1,0}$, the system undergoes a Hopf bifurcation at E^*, as illustrated in Figure 4. However, when the critical value is exceeded, the equilibrium point loses stability and becomes unstable, resulting in the emergence of a periodic solution around E^*, as shown in Figure 5.

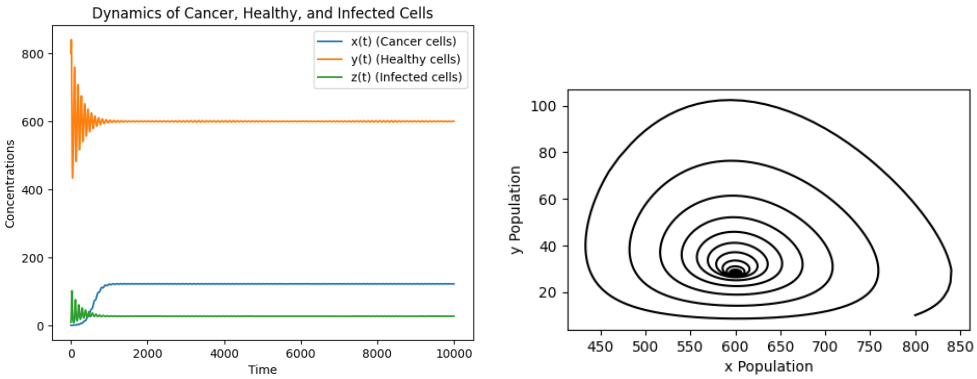

Figure 1: When $\tau_1 = \tau_2 = 0$ for Case I, E^* of the system Eqn. (2.1) is locally asymptotically stable. Left: All the concentrations (Cancer- Healthy- Infected Cells) converge to the positive equilibrium value. Right: Phase diagram of the system (2.1).

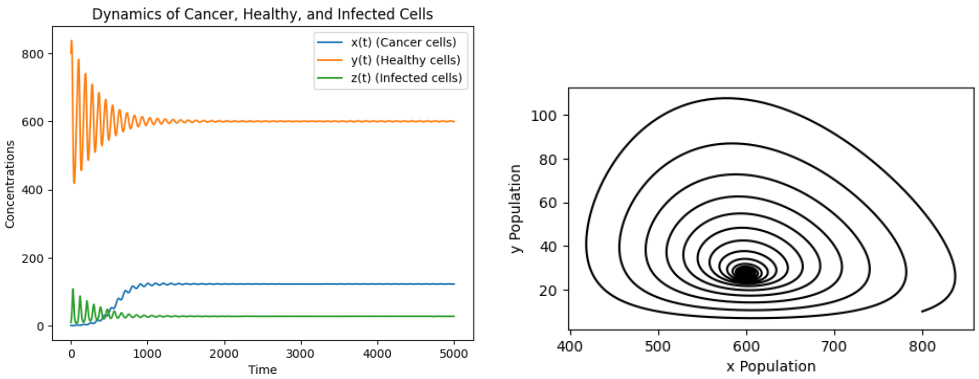

Figure 2: When $\tau_1 = 1$ for Case II, E^* of the system Eqn. (2.1) is locally asymptotically stable. Left: All the concentrations (Cancer- Healthy- Infected Cells) converge to the positive equilibrium value. Right: Phase diagram of the system (2.1)

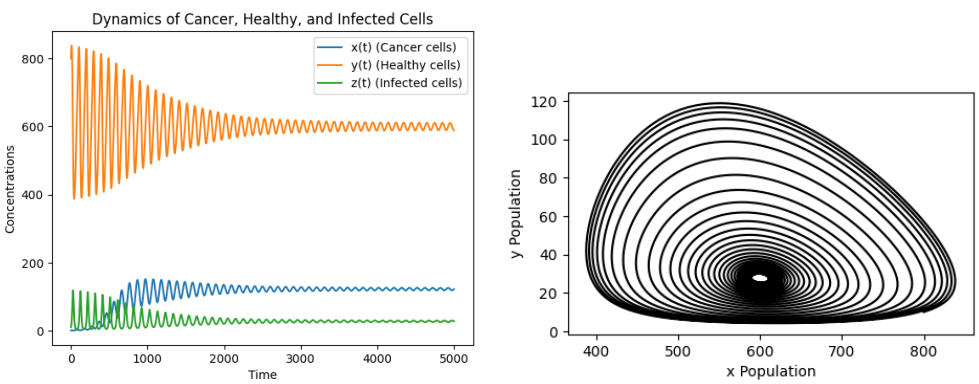

Figure 3: When $\tau_1 = 2$ for Case II, E^* of the system Eqn. (2.1) is locally asymptotically stable. Left: All the concentrations (Cancer- Healthy- Infected Cells) converge to the positive equilibrium value. Right: Phase diagram of the system (2.1)

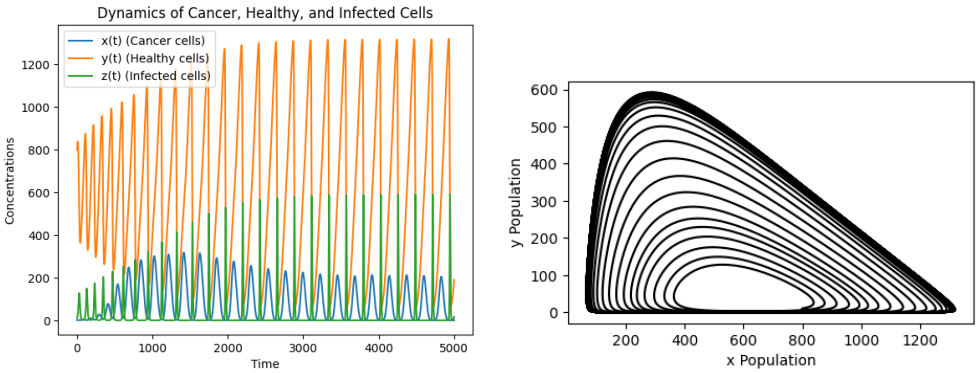

Figure 4: When $\tau_1 = 2.72$ for Case II, the system Eqn. (2.1) undergoes a Hopf bifurcation. Left: The time plot of all concentrations (cancer, healthy, and infected cells) displays periodic oscillations. Right: Phase diagram of the system (2.1)

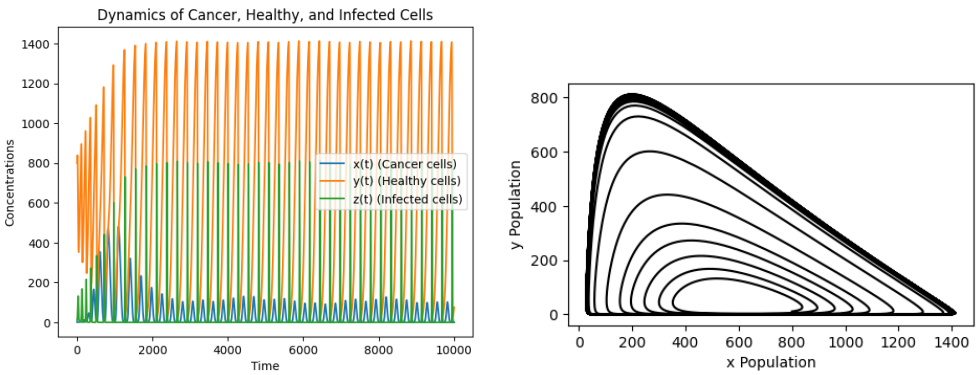

Figure 5: When $\tau_1 = 3$ for Case II, E^* of the system Eqn. (2.1) is locally asymptotically stable. Left: The time plot of all concentrations (cancer, healthy, and infected cells) displays periodic oscillations. Right: Phase diagram of the system (2.1)

For Case III, where $\tau_1 = 0$ and $\tau_2 > 0$, we adjust the parameter b_2 to 0.00055, while maintaining other parameters as in the previous case. This results in a new equilibrium point $E^*(252.52525, 545.45455, 20.2020)$. With these parameters, ω_0 is calculated as 0.024796 and $\tau_{2,0}$ as 7.2680. For τ_2 values below the critical threshold $\tau_{2,0}$, the populations of cancer cells, healthy cells, and infected cells exhibit oscillatory behavior before stabilizing at the equilibrium point. As predicted by Theorem 2.2, the equilibrium point E^* is locally asymptotically stable for τ_2 within the interval $(0, \tau_{2,0})$ but becomes unstable when $\tau_2 \geq \tau_{2,0}$, as demonstrated in Figures 6, 7, and 8.

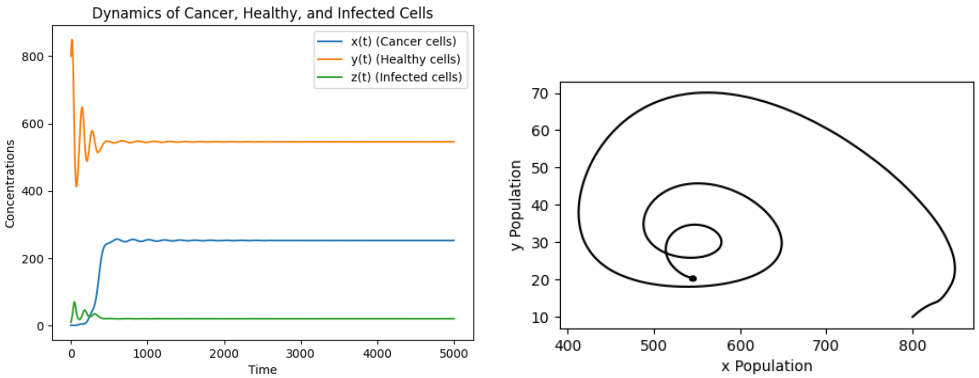

Figure 6: When $\tau_2 = 5$ for Case III, E^* of the system Eqn. (2.1) is locally asymptotically stable. Left: All the concentrations (Cancer- Healthy- Infected Cells) converge to the positive equilibrium point E^*. Right: Phase diagram of the system (2.1)

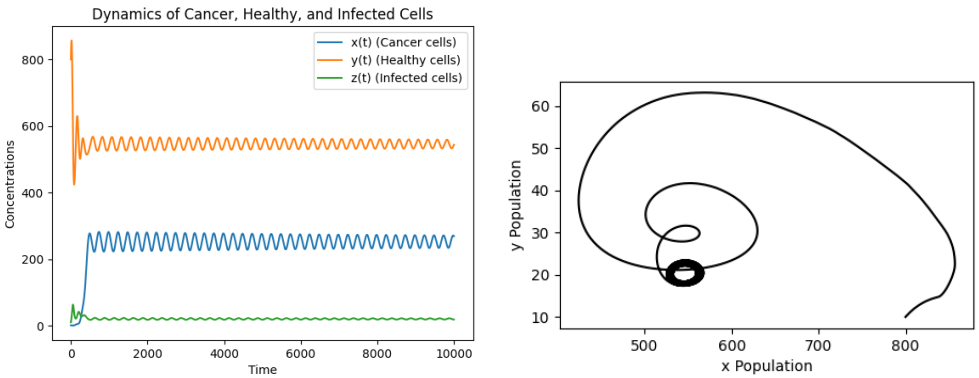

Figure 7: When $\tau_2 = 7.2$ for Case III, the system Eqn. (2.1) undergoes a Hopf bifurcation. Left: The time plot of all concentrations (cancer, healthy, and infected cells) displays periodic oscillations. Right: Phase diagram of the system (2.1)

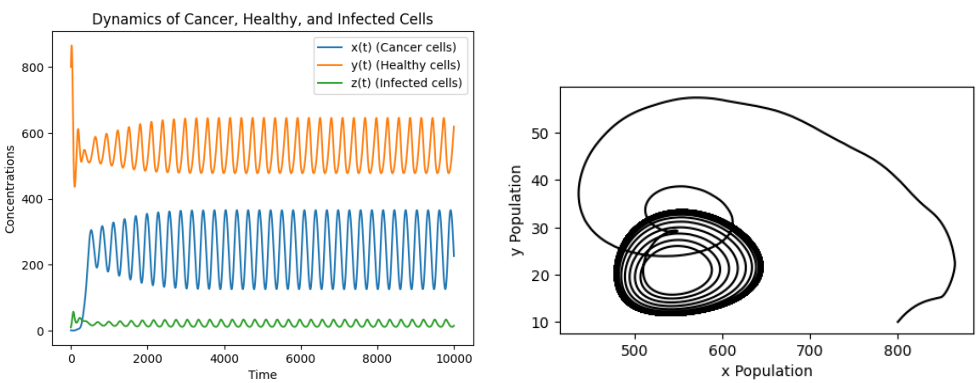

Figure 8: When $\tau_2 = 10$ for Case III, the system Eqn. (2.1) undergoes a Hopf bifurcation. Left: The time plot of all concentrations (cancer, healthy, and infected cells) displays periodic oscillations. Right: Phase diagram of the system (2.1)

For Case IV, τ_2 is fixed at 15, while other parameters remain consistent with Case I. The equilibrium point is $E^*(122.4489796, 600.0, 27.551020)$. Due to the complexity of Equation (2.36), its roots were determined numerically, yielding $\omega_0 = 0.0207554$ and $\tau^*_{1,0} = 16.460636$. The system exhibits local asymptotic stability for τ_1 values below the critical threshold $\tau^*_{1,0}$. Conversely, when $\tau_1 \geq \tau^*_{1,0}$, a Hopf bifurcation occurs, as illustrated in Figures 9, 10, and 11.

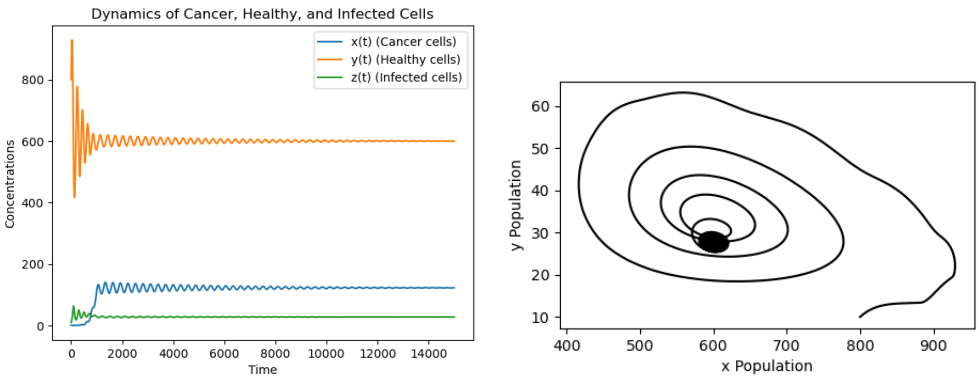

Figure 9: When $\tau_2 = 15$ and $\tau_1 = 13$ for Case IV, E^* of the system Eqn. (2.1) is locally asymptotically stable for Case IV. Left: All the concentrations (Cancer- Healthy- Infected Cells) converge to the positive equilibrium value. Right: Phase diagram of E^*

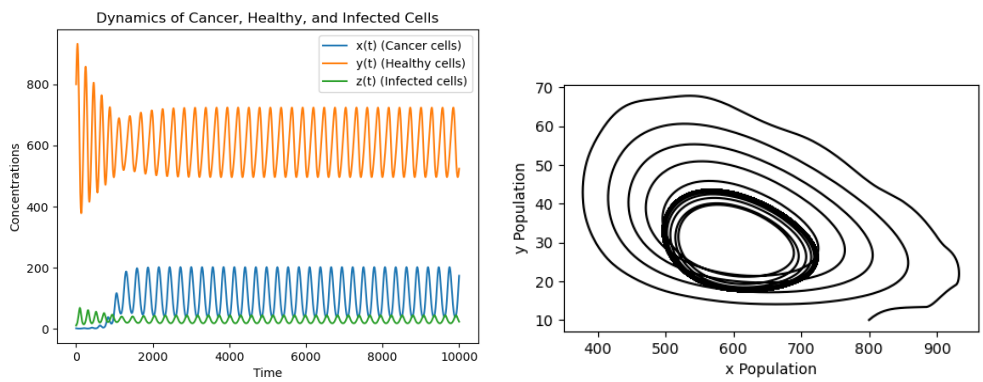

Figure 10: When $\tau_2 = 15$ and $\tau_1 = 16.460636$ for Case IV, the system Eqn. (2.1) undergoes a Hopf bifurcation. Left: The time plot of all concentrations (cancer, healthy, and infected cells) displays periodic oscillations. Right: Phase diagram of the system (2.1)

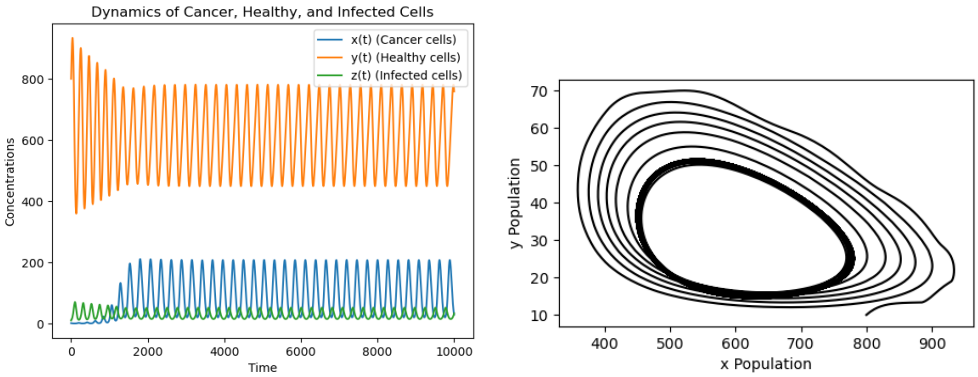

Figure 11: When $\tau_2 = 15$ and $\tau_1 = 18$ for Case IV, the system Eqn. (2.1) undergoes a Hopf bifurcation. Left: The time plot of all concentrations (cancer, healthy, and infected cells) displays periodic oscillations. Right: Phase diagram of the system (2.1)

The model incorporates a latent infection phase, assuming that infected cells undergo a period of latency before being actively productive. Two time delays are introduced to capture this process: τ_1 represents the time between viral entry and the establishment of latent infection (i.e., viral DNA integration), while τ_2 represents the time from viral entry to the onset of viral production.

4. Conclusion

This study investigates the dynamics of an HIV-associated cancer model that incorporates two time delays to accurately represent the incubation and replication phases of viral infection. The model captures the intricate interactions between cancer cells, healthy cells, and HIV-infected cells, including immune responses. We analyze the system's stability and derive the conditions for Hopf bifurcations through characteristic equation analysis for various delay scenarios. Numerical simulations complement the theoretical findings, demonstrating the impact of delay parameters on system dynamics.

The model incorporates a latent infection phase, assuming that infected cells undergo a period of latency before being actively productive. Two time delays are introduced to capture this process: τ_1 represents the time between viral entry and the establishment of latent infection (i.e., viral DNA integration), while τ_2 represents the time from viral entry to the onset of viral production. These time delays lead to periodic oscillations after critical thresholds, indicating a nonlinear fluctuation in the populations of cancer cells, healthy cells, and HIV-infected cells. Biologically, this suggests a periodic exacerbation and remission cycle, potentially linked to immune response dynamics and viral activity.

The two time delays addressed are of critical importance for the optimization of treatment strategies, representing stages in the viral life cycle where HIV either remains latent or begins active replication. By identifying and targeting these stages, particularly during replication delay, antiretroviral therapies can disrupt viral production before reaching critical levels.

The results highlight the importance of understanding the delay parameters to better predict how the system behaves over time. A deeper understanding of system dynamics could inform the development of targeted treatment strategies that disrupt specific stages of the viral life cycle and account for delays in immune response. Future research should explore the impact of drug therapies, co-infections, and more intricate immune system interactions on the model's outcomes. By expanding the complexity of the model, we can gain valuable insight into HIV-associated cancers and refine prevention and treatment strategies.

References

1. K. Antman and Y. Chang, *Kaposi's sarcoma*, New England Journal of Medicine, vol. 342, no. 14, pp. 1027–1038, 2000.

2. Y. Chang, E. Cesarman, M. S. Pessin, F. Lee, J. Culpepper, D. M. Knowles, and P. S. Moore, *Identification of herpesvirus-like DNA sequences in AIDS-associated Kaposi's sarcoma*, Science, vol. 266, no. 5192, pp. 1865–1869, (1994).

3. S. Khajanchi, D. K. Das, and T. K. Kar, *Dynamics of tuberculosis transmission with exogenous reinfections and endogenous reactivation*, Physica A: Statistical Mechanics and its Applications, vol. 497, pp. 52–71, (2018).

4. A. Razeah, E. Dahy, E. K. Elnahary, and S. A. Azoz, *Stability of HIV-1 Dynamics Models with Viral and Cellular Infections in the Presence of Macrophages*, Axioms, vol. 12, no. 7, p. 617, (2023).

5. S. Khajanchi, S. Bera, and T. K. Roy, *Mathematical analysis of the global dynamics of a HTLV-I infection model, considering the role of cytotoxic T-lymphocytes*, Mathematics and Computers in Simulation, vol. 180, pp. 354–378, (2021).

6. D. K. Das, S. Khajanchi, and T. K. Kar, *Transmission dynamics of tuberculosis with multiple re-infections*, Chaos, Solitons & Fractals, vol. 180, p. 109450, (2020).

7. J. Lou, T. Ruggeri, and C. Tebaldi, *Modeling cancer in HIV-1 infected individuals: equilibria, cycles and chaotic behavior*, Mathematical Biosciences & Engineering, vol. 3, no. 2, pp. 313–324, (2006).

8. J. Lou and T. Ruggeri, *A time delay model about AIDS-related cancer: equilibria, cycles and chaotic behavior*, Ricerche di Matematica, vol. 56, pp. 195–208, (2007).

9. U. Foryś and J. Polewczak, *A delay-differential equation model of HIV related cancer-immune system dynamics*, Mathematical Biosciences and Engineering, vol. 8, pp. 627–644, (2011).

10. A. M. Elaiw and N. A. Almuallem, *Global dynamics of delay-distributed HIV infection models with differential drug efficacy in cocirculating target cells*, Mathematical Methods in the Applied Sciences, vol. 39, pp. 4–31, (2016).

11. S. S. Chen, C. Y. Cheng, and Y. Takeuchi, *Stability analysis in delayed within-host viral dynamics with both viral and cellular infections*, Journal of Mathematical Analysis and Applications, vol. 442, pp. 642–672, (2016).

12. H. Pourbashash, S. S. Pilyugin, P. De Leenheer, and C. McCluskey, *Global analysis of within host virus models with cell-to-cell viral transmission*, Discrete and Continuous Dynamical Systems - Series B, vol. 19, no. 10, pp. 3341–3357, (2014).

13. A. S. Perelson, D. E. Kirschner, and R. De Boer, *Dynamics of HIV infection of CD4+ T cells*, Mathematical Biosciences, vol. 114, no. 1, pp. 81–125, (1993).

14. R. V. Culshaw and S. Ruan, *A delay-differential equation model of HIV infection of CD4+ T-cells*, Mathematical Biosciences, vol. 165, no. 1, pp. 27–39, (2000).

15. P. Gupta and R. Balachandran, *Cell-to-cell transmission of human immunodeficiency virus type 1 in the presence of azidothymidine and neutralizing antibody*, Journal of Virology, vol. 63, pp. 2361–2365, (1989).

16. M. L. Diegel and P. A. Moran, *Regulation of HIV production by blood mononuclear cells from HIV-infected donors: II. HIV-1 production depends on T cell-monocyte interaction*, AIDS Research and Human Retroviruses, vol. 9, pp. 465–473, (1993).

17. R. D. Schrier, J. A. McCutchan, and C. A. Wiley, *Mechanisms of immune activation of human immunodeficiency virus in monocytes/macrophages*, Journal of Virology, vol. 67, pp. 5713–5720, (1993).

18. D. S. Callaway and A. S. Perelson, *HIV-1 Infection and low steady state viral loads*, Bulletin of Mathematical Biology, vol. 64, pp. 29–64, (2002).

19. J. Duarte, C. Januário, N. Martins, C. Correia, and J. Sardanyés, *Optimal homotopy analysis of a chaotic HIV-1 model incorporating AIDS-related cancer cells*, Numerical Algorithms, vol. 77, pp. 261–288, (2018).

20. J. A. Levy, *HIV and the Pathogenesis of AIDS*, Springer, New York, (1999).

21. Q. Sheng and D. Chanying, *Nonlinear Models in Immunity*, Shanghai Science & Technology Education Press, Shanghai, China, (1998).

22. J. L. Spouge, R. I. Shrager, and D. S. Dimitrov, *HIV-1 infection kinetics in tissue cultures*, Mathematical Biosciences, vol. 138, no. 1, pp. 1–22, (1996).

23. S. P. Layne, M. J. Merges, M. Dembo, J. L. Spouge, and P. L. Nara, *HIV requires multiple gp120 molecules for CD4-mediated infection*, Nature, vol. 346, no. 6281, pp. 277–279, (1990).

Rukiye Kara,
Department of Mathematics,
Mimar Sinan Fine Arts University,
Turkey.
E-mail address: rukiye.kara@msgsu.edu.tr